1 Trajectory Model

1.1 Forces and the Equation of Motion

This section will develop a simple, 1-dimensional model of the dynamics of droplets dominated by electrostatic forces. Treating a droplet as a particle, with radius R_d, the equation of motion of charged droplets center of mass as it translates vertically along the central axis of a finite square charged dielectric sheet is given by

$$my'' = -\mathbf{F}_D - \mathbf{F}_E, \quad y(0) = R_d, \quad y'(0) = U_0, \tag{1}$$

where m is the droplet mass, $y'' = \frac{d^2y}{dt^2}$ is the droplet acceleration, $\mathbf{F}_D$ is the drag force, and $\mathbf{F}_E$ is the electrostatic force. The initial conditions are such that, when the $\mathbb{B}$o is suddenly reduced at the start of the drop tower experiment, the droplet jumps with initial velocity U_0 from its 1-g resting position R_d at $t = 0$. The signs of the forces on the right side of Equation 1 indicate that they act in the opposite direction of the droplet motion. We need to specify models for the various forces in this equation to begin our analysis of the droplet dynamics.

With the assumption of an intermediate range of Reynolds numbers $\mathbb{R}e \equiv \frac{2UR_d}{\nu}$, $1 \leq \mathbb{R}e \leq 5000$ then the force of drag acting on the droplet will be quadratic,

$$\mathbf{F}_D = \frac{1}{2}C_D\rho A y'^2,$$

where C_D is the drag coefficient, ρ is the density of the sorrounding fluid medium (air, in this case), and A is the frontal area of the droplet. For

1

this range of Reynolds numbers it is appropriate to approximate the drag coefficient by the well known Abraham correlation [1]

$$C_D = \frac{24}{9.06^2} \left(1 + \frac{9.06}{\sqrt{\mathbb{R}\mathrm{e}}} \right)^2 .$$

Modeling the electrostatic force is somehwhat more involved, but we will start with the standard electrohydrodynamic (EHD) approximation [2] as our model, and further simplify where possible. Under a DC electric field, we assume that the real part of the dielectric permitivity ϵ, $Re\langle\epsilon\rangle \approx$ constant. We also assume that electric currents are small enough that the effects of magnetic fields can be neglected. The validity of this assumption rests on the size of the characteristic time scale for electrical phenomena $\tau_e = \epsilon\epsilon_0/\sigma_e \ll 1$, where τ_e is the ratio of absolute dielectric permittivity $\kappa = \epsilon\epsilon_0$, to conductivity σ_e, of the medium. This characteristic time τ_e is also known as the relaxation time, and is a measure of how quickly the polarization of a dielectric responds to a change in electric field. Given the respective conductivity, and permittivity of extremely-pure water ($\kappa \sim 80$, $\sigma_e = 18.2 \times 10^6$ Ωcm) [3], we estimate $\tau_e \approx 4 \times 10^{-6}$ s. The relaxation time for the common distilled water that is actually used in the droplet experiments is undoubtedly even shorted (due to the presence of solvated ions). Neglecting the effects of a electric double layer on hydration of ions (in the water or the ambient atmosphere) due to the reletively massive size of the droplets studied, then the assumption of small relaxation time further implies that the free charge present in the droplets will remain approximately constant during the typical time interval of a low-gravity experiment.

Supposing that electrical forces acting on free charges and dipoles in a fluid are transferred directly to the fluid itself, then this overall electrical body force will be the the divergence of the Maxwell stress tensor τ_m, by

$$\mathbf{F}_E = \nabla \cdot \tau_m = \nabla \cdot \left(\epsilon\epsilon_0 \mathbf{E}\mathbf{E} - \frac{1}{2}\epsilon\epsilon_0 \mathbf{E} \cdot \mathbf{E}\delta \right),$$

where $\mathbf{F}_E$ is the electric body force per unit volume, and δ is the delta function. The product of the electric field vectors is the dyadic product.

The classical Korteweg-Helmholtz force density formulation of the Maxwell stress tensor is usually expressed as [4]

$$\mathbf{F}_E = \rho_f \mathbf{E} + \frac{1}{2}\left| E \right|^2 \nabla\epsilon - \nabla\left(\frac{1}{2}\rho\left(\frac{\partial \epsilon}{\partial \rho} \right)_T \left| E \right|^2 \right). \tag{2}$$

The first term in this expression, equivalently written as $q\mathbf{E}$, is the well known Coulombic force or electrophoretic force, which arises from the presence of free charge in an external electric field. We expect this term to dominate the electric force in a DC field. The second term is the force arising from polarization stresses due to a nonuniform field acting across a gradient in permittivity. This force is widely termed the dielectrophoretic force (DEP). The third term describes forces due to electrostriction. It has been noted by Melcher and Hurwitz that the electrostriction term is the gradient of a scalar and can thus be cannononically lumped togeather with the hydrostatic pressure for incompressible fluids) [5]; we neglect it in our analysis.

It is common to approximate the polarization stress by idealizing the droplet as a simple dipole using the effective dipole moment method first

suggested by Pohl in 1958 [6]. This approach has been related back to the force density by the volumetric integration of the force density with the substitution of a Taylor series expansion of $\mathbf{E}$ in the limit of a small radial gradient of the field within the dielectric sphere [7]. The DEP force is related to the dipole moment (induced or permanent) of polarizable media which has a tendency to align the dipole with the electric field. If there is a gradient in the field then for a finite separation of charge one end of the dipole will feel a stronger electric field than the other, resulting in a net force. Whether the force is positive or negative in the direction of the electric field gradient depends on the difference of dielectric permittivites between the fluids, rather than on the polarity of $\mathbf{E}$ itself. In principle an external electric field will tend to induce a dipole in a dielectric material, but if the field is spatially uniform there is no gradient in the field and the forces felt by the dipoles are symmetric and thus there is no net force. The dipole moment of a spherical linear-dielectric particle immersed in a dielectric medium is given by

$$\mu = V_d\mathbf{P} = \frac{4}{3}\pi R_d^3\mathbf{P}, \tag{3}$$

where $\mathbf{P} = (\kappa_1 - 1)\,\epsilon_0\mathbf{E} = \chi_e\epsilon_0\mathbf{E}$ is the polarization moment, and R_d is the particle radius, $\kappa_1 = \frac{\epsilon}{\epsilon_0}$ being the relative dielectric constant of the external medium (air in this case), $\chi_e = \kappa_1 - 1$ being the electric susceptibility of the dielectric medium. The excess polarization $\mathbf{P}_e$, in the sphere is given by

$$\mathbf{P}_e = (\kappa_2 - \kappa_1)\,\epsilon_0\mathbf{E} = \frac{3\kappa_1}{\kappa_2 + 2\kappa_1}\mathbf{E}, \tag{4}$$

4

where κ_2 is the relative dielectric constant of the spherical particle. Taking together Equations 3, and 4 the effective dipole moment of the particle is given by

$$\mu = 4\pi R_d^3 \left(\frac{\kappa_2 - \kappa_1}{\kappa_2 + 2\kappa_1} \right) \kappa_1 \epsilon_0 \mathbf{E}, \qquad (5)$$

and the force felt by the dipole is

$$
\begin{aligned}
\mathbf{F}_{DEP} &= (\mathbf{P}_e \cdot \nabla) \mathbf{E} \\
&= 2\pi R_d^3 \kappa_1 \epsilon_0 K \nabla E^2, \qquad (6)
\end{aligned}
$$

where it is nice to use the simplifying shorthand $K = \frac{\kappa_2 - \kappa_1}{\kappa_2 + 2\kappa_1}$, which is also known as the Clausius-Mossotti factor. In cases where $K < 0$, or $K > 0$ the particle will be repelled or attracted to regions of strong field respectively. In our experiment, taking the relative dielectric constants to be $\kappa_1 \approx 1$ and $\kappa_2 \approx 80$, the Clausius-Mossotti factor $K \approx 0.96$. It is important to note that the equivalent dipole approximation critically requires an assumption of small physical scale of the particle relative to the lengthscale of nonuniformity of the field, which in this case we take to be the length of the charged superhydrophobic surface ($L = 25$ mm $\gg a \approx 2.5$ mm).

When the droplet is close to the dielectric surface, the free charge on the droplet will tend to induce polarization of the dielectric, perturbing the electric field. The polarization bound charge in the dielectric will be of the opposite sign of the free droplet charge and thus there will be a force of attraction. This so-called image force is a correction to the Colomb force due to the external electric field only, and can be found by the method of images

[8]. The image force $\mathbf{F}_I$, is given by

$$\mathbf{F}_I = \frac{kq^2}{16\pi\epsilon_0}y^{-2}\hat{\mathbf{j}}, \tag{7}$$

where the factor k is a function of the dielectric surface susceptibility $k = \frac{\chi_e}{\chi_e+2}$, and $\hat{\mathbf{j}}$ is a unit vector normal to the dielectric surface.

By substituting Equations 6, 7 into Equation 2 we have

$$\begin{aligned}
\mathbf{F}_E &= q\mathbf{E} + \mathbf{F}_{DEP} + \mathbf{F}_I \\
&= q\mathbf{E} + \frac{kq^2}{16\pi\epsilon_0}y^{-2}\hat{\mathbf{j}} + 2\pi R_d^3\kappa_1\epsilon_0 K\nabla E^2,
\end{aligned}$$

and the 1-D governing equation becomes

$$my'' = -\tfrac{1}{2}C_D\rho Ay'^2 - qE - \frac{kq^2}{16\pi\epsilon_0}y^{-2} - 2\pi R_d^3\kappa_1\epsilon_0 K\nabla E^2,$$

$$y(0) = R, \ y'(0) = U_0. \tag{8}$$

By comparing DEP and Coulombic terms in Equation 8, we note that a condition to neglect the DEP term is

$$\frac{q}{\kappa_2\epsilon_0 K R_d^2 E_0} \gg 1$$

As this condition likely holds in our experiments we henceforth neglect the DEP force in our analysis. There is some physical intuition to support this conclusion as well. The dielectric displacement, $\mathbf{D} = \kappa\epsilon_0\mathbf{E}$ of a water droplet in air is very high due to its large relative dielectric constant. This implies that the field strength within the droplet is about 2 orders of magnitude

6

smaller than in the surrounding medium (which is essentially the same as a vacuum from a dielectric standpoint), thus it is not particularly inaccurate to model the dielectric volume of a droplet as a conductive shell (an equipotential), with zero field in its interior. As an aside, in treating the droplet as an ideal conductor we note that in our specific case the electrostatic force is not a body force *per se* as the electric field is acting on charges on the surface of the conductor.

1.2   The Electric Field

If we consider the charged dielectric surface of our experiments to be a square sheet of charge lying in the xz-plane with width L, the symmetry of the problem happily lets us obtain the y-component of the electric field $\mathbf{E}$ by direct integration. In particular it is easy to constuct the electric field due to a finite plane of charge by superposition of the electric fields of a series of line charges. By symmetry the electric field points along the y-axis; for a point along the y-axis the position vector is $\mathbf{r} = \left(x^2 + y^2\right)^{1/2} \hat{\mathbf{r}}$ to the center of a line charge in the xz-plane. The y-component of $d\mathbf{E}$ is found by $dE_r = dE_y \cos \theta = dE_y y / r$, where θ is the angle made between the y-axis and the position vector $\mathbf{r}$. If the charge in a line element, dx is $\sigma L dx$, where σ is the average surface charge density, the electric field of a line charge is given by [8]

$$dE_r = \frac{k\sigma L dx}{4\pi\epsilon_0 r \sqrt{r^2 + L^2/4}}.$$

The y-component of the electric field E_y, is then

$$E_y = \frac{\sigma L y}{4\pi\epsilon_0} \int_{-L/2}^{L/2} \frac{1}{(y^2 + x^2)\sqrt{y^2 + x^2 + L^2/4}} dx.$$

With some substitutions this can be integrated to obtain an expression for the electric field in terms of y,

$$E_y = \frac{\sigma}{\pi\epsilon_0} \tan^{-1}\left(\frac{L^2}{y\sqrt{2L^2 + y^2}}\right). \tag{9}$$

We note that this model of the electric field will be poor except in cases where $y \ll L$, $R_d \ll L$, which will be true for cases of large drops very close to the dielectric surface. For accurate models of the field in this case we likely would need to solve Laplace's equation for the electric potential φ

$$-\nabla^2\varphi = 0,$$

numerically using finite element methods.

By taking Taylor series expansions in large and small limits we can intuit a bit about the behavior of this field. In the limit $L \to \infty$, $y \ll L$ the argument of the function tends towards infinity and

$$\lim_{x\to\infty} \tan^{-1}(x) = \frac{\pi}{2},$$

and thus

$$E_y \approx \frac{\sigma}{4\pi\epsilon_0} = E_0 \qquad y \ll L, \tag{10}$$

where E_0 is the characteristic electric field given by $E_0 = \frac{\sigma}{4\pi\epsilon_0}$. This field

8

is constant, and equivalent to the electric field due to an infinite plane of charge. In the limit of $y \gg L$, the argument of the arctangent function can be approximated by

$$\frac{L^2}{2y \left(2L^2 + 4y^2\right)^{1/2}} = \frac{L^2}{4y^2 \left(1 + L^2/2y^2\right)^{1/2}} \approx \frac{L^2}{4y^2}.$$

For small x, $\tan^{-1}(x) \sim x$ and we thus find the familiar electric field due to a point charge

$$E_y \approx L^2 E_0 y^{-2} \qquad y \gg L. \tag{11}$$

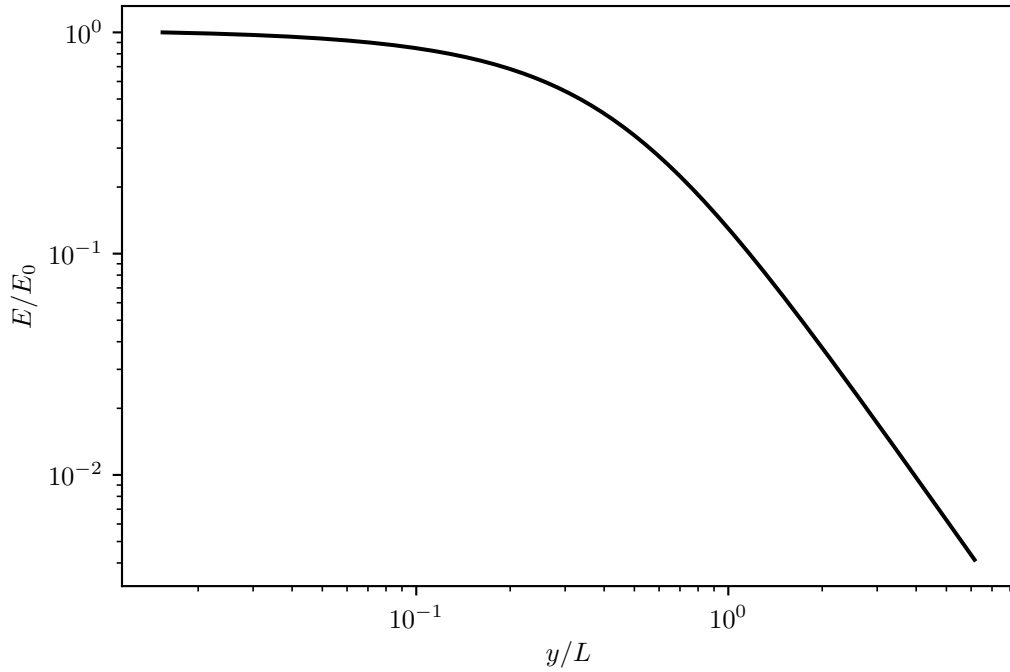Both of these regimes can be clearly seen in the plot of E_y shown in Figure 1.

Figure 1: A log-log plot of the magnitude of the non-dimensional electric field, E_y.

1.3 Scaling

The equation of motion is non-linear, non-homogeneous and is best solved numerically, but nevertheless we are curious if we can obtain approximate solutions to the equation analytically using perturbation methods. This is aided by non-dimensionalizing the governing equations, and seeing if any dimensionless groups exist, and whether any are particularly small or large, and whether any fortuitous opportunities for simplification appear. Introducing the scaled variables

$$\bar{t} = \frac{t}{t_c}, \qquad \bar{y} = \frac{y}{y_c},$$ (12)

where y_c and t_c are characteristic length and time scales respectively, and using the coordinate transformation $y(0) - R = 0$, the governing equation becomes

$$\bar{y}'' = -\frac{1}{2}\frac{C_D \rho A y_c}{m}\bar{y}'^2 - \frac{qE_0 t_c^2}{m y_c}\bar{E}(\bar{y}) - \frac{kq^2 t_c^2}{16\pi\epsilon_0 R^2 m y_c}\left(\frac{y_c}{R}\bar{y} + 1\right)^{-2},$$

$$\bar{y}(0) = 0, \ \bar{y}'(0) = \frac{U_0 t_c}{y_c}.$$ (13)

We note the existence of several dimensionless groups

$$\mathbf{\Pi}_1 = \frac{C_D \rho A y_c}{2m}, \quad \mathbf{\Pi}_2 = \frac{qE_0 t_c^2}{m y_c}, \quad \mathbf{\Pi}_3 = \frac{kq^2 t_c^2}{16\pi\epsilon_0 R^2 m y_c}, \quad \mathbf{\Pi}_4 = \frac{y_c}{R}, \quad \mathbf{\Pi}_5 = \frac{U_0 t_c}{y_c}.$$

1.3.1 Inertial Electro-Image Limit

In the limit of small y and t we expect inertia to scale as Coulombic and image force. In this limit we can approximate the electric field as the constant, E_0. One possible characteristic length scale is $y_c \sim R_d$, however this ultimately

10

is a poor choice. With $y_c \sim U_0 t_c$ and picking t_c such that Coulombic force is $\mathcal{O}(1)$, the intrinsic scales become

$$t_c \sim \frac{mU_0}{qE_0}, \quad y_c \sim \frac{mU_0^2}{qE_0}.$$

With these scales the governing equation then becomes

$$\bar{y}'' = -1 - \mathbb{Im} \left(\mathbb{Eu} \bar{y} + 1 \right)^{-2},$$

$$\bar{y}(0) = 0, \ \bar{y}'(0) = 1. \tag{14}$$

with

$$\mathbb{Im} \equiv \frac{kq}{16\pi\epsilon_0 R_d^2 E_0} = \mathbf{\Pi}_3, \quad \mathbb{Eu} \equiv \frac{mU_0^2}{qE_0 R_d} = \mathbf{\Pi}_4,$$

where $\mathbb{Im}$ is the Image number, and denotes the ratio of image forces to the Coulombic force of the unperturbed field, and where $\mathbb{Eu}$ is the electrostatic Euler number, and is a ratio of inertia to electrostatic force.

1.3.2 Inertial Electro-Viscous Limit

In the limit of large y and t we expect droplet inertia to scale as Coulombic force and drag. In this limit we approximate the electric field as $E \approx y_c^2 E_0 y^{-2}$. In this case there are several (obvious) possible choices of scales:

1. $y_c \sim U_0 t_c$, and make Coulomb force $\mathcal{O}(1)$.

2. $y_c \sim L$, $t_c \sim \frac{L}{U_0}$ (however, this makes Equation 13 singular).

3. $y_c \sim L$, $t_c \sim \left(\frac{Lm}{qE_0} \right)^{1/2}$.

4. $y_c \sim L$, and make Coulomb force $\mathcal{O}(1)$.

We prefer the approach with the greatest physical simplicity, fewest Pi terms, and that has homogeneous initial conditions. We choose Case 1, where the intrinsic scales are given by

$$t_c \sim \frac{R_d^2}{L^2} \frac{4\pi m U_0}{q E_0}, \quad y_c \sim \frac{R_d^2}{L^2} \frac{4\pi m U_0^2}{q E_0}.$$

With this scaling the non-dimensional governing equation is

$$\bar{y}'' = -\mathbb{D}\mathrm{g}\mathbb{E}\mathrm{u}_+ \bar{y}'^2 - (\mathbb{E}\mathrm{u}_+ \bar{y} + 1)^{-2},$$

$$\bar{y}(0) = 0, \ \bar{y}'(0) = 1 \tag{15}$$

where we call $\mathbb{D}\mathrm{g}$ the drag number, $\mathbb{D}\mathrm{g} \equiv \frac{C_D \rho_a}{\rho_l} = \boldsymbol{\Pi}_1 \mathbb{E}\mathrm{u}_+^{-1}$ and $\mathbb{E}\mathrm{u}_+ = 4\pi \frac{R_d^2}{L^2} \mathbb{E}\mathrm{u}$.

1.4 Asymptotic Estimates

1.4.1 Inertial Electro-Image Limit

The alternate scalings of the equation of motion given by Equations 14, and 15 are weakly non-linear differential equations in the sense that they reduce to linear equations as the parameter $\mathbb{E}\mathrm{u} \to 0$. If we take $\mathbb{E}\mathrm{u}$ to be a small parameter ϵ, we can find an asymptotic approximation to the solution of the non-linear equation by means of a regular perturbation. In this case we use the naive expansion

$$\bar{y}(\bar{t}) \sim \bar{y}_0(\bar{t}) + \epsilon \bar{y}_1(\bar{t}) + \epsilon^2 \bar{y}_2(\bar{t}) \ldots \epsilon^n \bar{y}_n(\bar{t}).$$

By substitution of the expansion (and its derivatives) into the differential equation, and equating terms by order, and using the notation $\alpha = \mathbb{I}\mathrm{m}$ (this being the equation scaled in the small-times limit), we first find the $\mathcal{O}(1)$, unperturbed, solution to the equation of motion to be

$$\bar{y}_0(\bar{t}) = \bar{t} + \frac{\bar{t}^2}{2}\left(-1-\alpha\right).$$

Looking at this solution it is evident that if we let $\alpha = 0$, the solution is the classical kinematic equation for projectile motion without drag under constant gravity, g_0. Continuing on with this procedure we find, (after some tedious computations, documented in Appendix ref) the higher order composite solutions to be

$$\bar{y}(\bar{t}) = \bar{t} + \frac{\bar{t}^2}{2}\left(-1-\alpha\right) + \epsilon\left(\frac{\alpha\bar{t}^3}{3} + \frac{\alpha\bar{t}^4}{12}\left(-1-\alpha\right)\right)$$
$$+\epsilon^2\left(-\frac{\alpha\bar{t}^4}{4} + \frac{\alpha\bar{t}^5}{60}\left(9+11\alpha\right) + \frac{\alpha\bar{t}^6}{360}\left(-9-20\alpha-11\alpha^2\right)\right) + \mathcal{O}(\epsilon^3) \quad .$$

In fact we, for somewhat arbitrary reasons, computed an $\mathcal{O}(\epsilon^5)$ accurate solution, but it is far to ugly to reprint here in its entirety. However, we plot these approximate short-time scaled solutions with varying values of the Image number, $\mathbb{I}\mathrm{m} = \alpha$ in Figure 2. These plots show a trend of decreasing time-of-flight (the time for the droplet to return to the origin, or complete a single "bounce"), and height at apoapse with increasing values of the Image number α. When $\alpha = 1$ the time of flight is exactly half of characteristic time scale in this regime. In the limit of small ϵ the trajectories collapse to the $\mathcal{O}(1)$ solution regardless of the Image number. In principle there is some
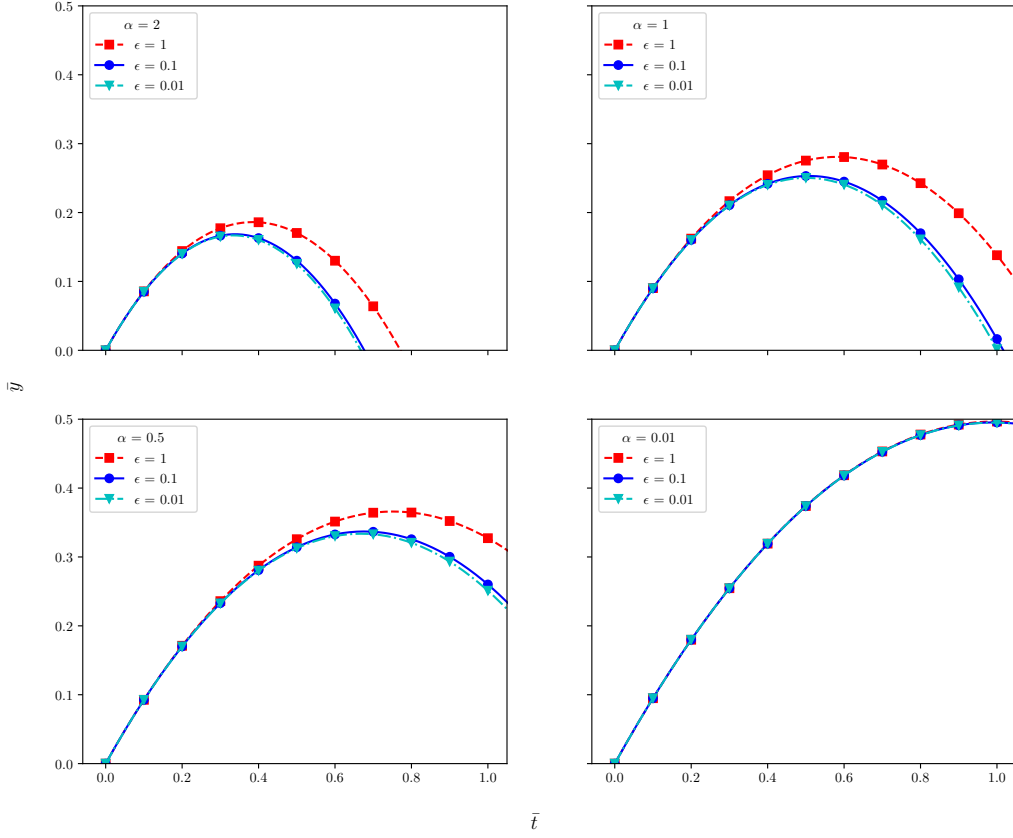
Figure 2: Non-dimensional droplet trajectories for various values of $\mathbb{E}u = \epsilon$, $\mathbb{I}m = \alpha$. The trajectory reduces to the classical $\mathcal{O}(1)$ solution for small values of α. It should be noted that despite what is implied by these plots α is not necessarily completely independent of ϵ, as they share q, and E_0 as common factors, $U_0 \sim R_d^2$, and $m \sim R_d^3$.

coupling between $\mathbb{E}u$ and $\mathbb{I}m$; notably this relationship does not depend on the electric field E_0 but on a charge to mass ratio. The effect of contact line hysteresis on the initial jump velocity U_0 will also tend to independently decohere the natural covariance between these parameters.

1.4.2 Inertial Electro-Viscous Limit

By similar arguments we find an asymptotic estimate of the trajectory in the long-times scaled regime. With $\epsilon = \mathbb{E}u_+$, where ϵ again is a small parameter, and $\beta = \mathbb{D}g$, the approximate solution is

$$\bar{y}(\bar{t}) = \bar{t} - \tfrac{\bar{t}^2}{2} + \epsilon \left(\tfrac{\bar{t}^3}{3} \left(1 + \beta \right) + \tfrac{\bar{t}^4}{12} \left(-1 - \beta \right) - \tfrac{\beta \bar{t}^2}{2} \right)$$

$$+\epsilon^2 \left(\tfrac{\bar{t}^4}{12} \left(-3 - 3\beta - 4\beta^2 \right) + \tfrac{\bar{t}^5}{60} \left(11 + 10\beta + 8\beta^2 \right) + \tfrac{\bar{t}^6}{360} \left(-11 - 10\beta - 8\beta^2 \right) + \tfrac{\beta^2 \bar{t}^3}{3} \right)$$

$$+\mathcal{O}(\epsilon^3)$$

This trajectory given by this solution is shown in Figure 3. If we assume a constant scale for the drag coefficient, $C_d \approx 0.5$, then the Drag number $\beta = \mathbb{D}g$ is approximately a constant $\beta \approx 6 \times 10^{-4}$ in all of our experiments. Again, the trajectory seemingly reduces to the classical $\mathcal{O}(1)$ solution for small values of of ϵ. We also note that the effect of drag is very slight, despite the fact that it appears explicitly in the $\mathcal{O}(1)$ solution [it does not]; the apoapse is very nearly equal to half the characteristic length scale. In practical terms this linearizing effect of small β may disappear if the fluid density is much less than that of water, as in our experiments.

By again applying a regular perturbation to the asymptotic solution with the expansion

$$\bar{t} \sim \bar{t}_0 + \epsilon \bar{t}_1 + \epsilon^2 \bar{t}_2 \ldots \epsilon^n \bar{t}_n,$$

and solving for the roots (that is, the times when $\bar{y} = 0$), we find an asymptotic estimate for the time-of-flight, t_f. The $\mathcal{O}(\epsilon^2)$ accurate time-of-flight
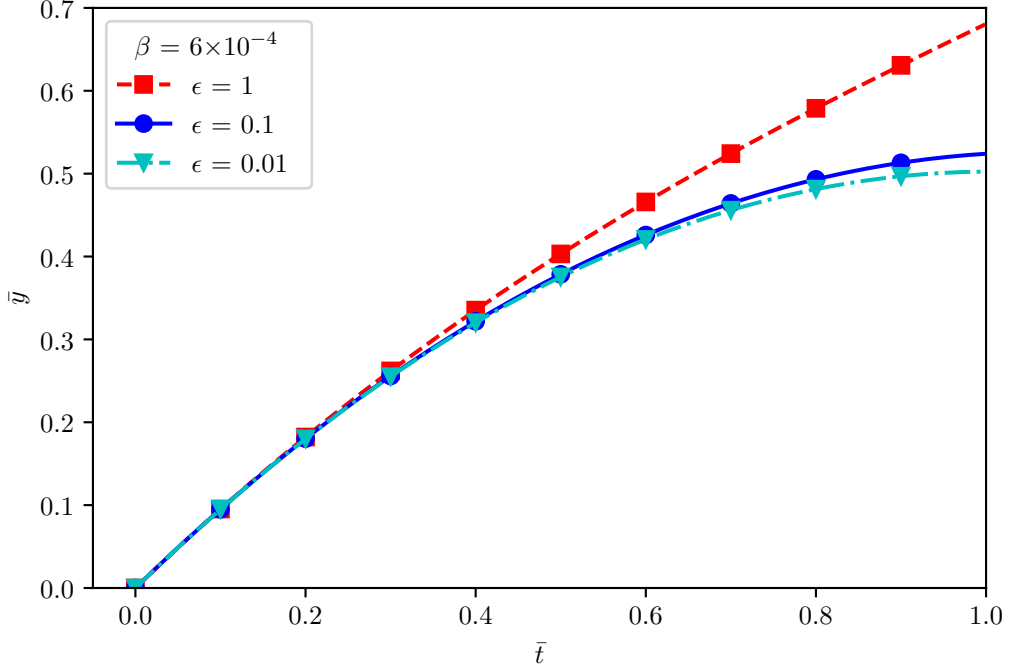
Figure 3: Non-dimensional droplet trajectories for various values of $\mathbb{E}u = \epsilon$.

estimate is given by

$$t_f = 2 + \epsilon \left(\frac{4}{3} - \frac{2\beta}{3} \right) + \epsilon^2 \left(\frac{4}{5} - \frac{4\beta}{3} + \frac{2\beta^2}{5} \right) + \mathcal{O}(\epsilon^3).$$

Substituting the experimental value of β we find the time-of-flight estimate for water droplets in air to be

$$t_f = 2 + 1.333\epsilon + 0.799\epsilon^2 + \mathcal{O}(\epsilon^3) \tag{16}$$

In Figure 4 we look at the effect of increasing values of $\mathbb{E}u_+$ on time-of-flight. We see that as ϵ grows to be no longer small, the time-of-flight grows rapidly, but this behavior appears to have an asymptote at a certain critical velocity
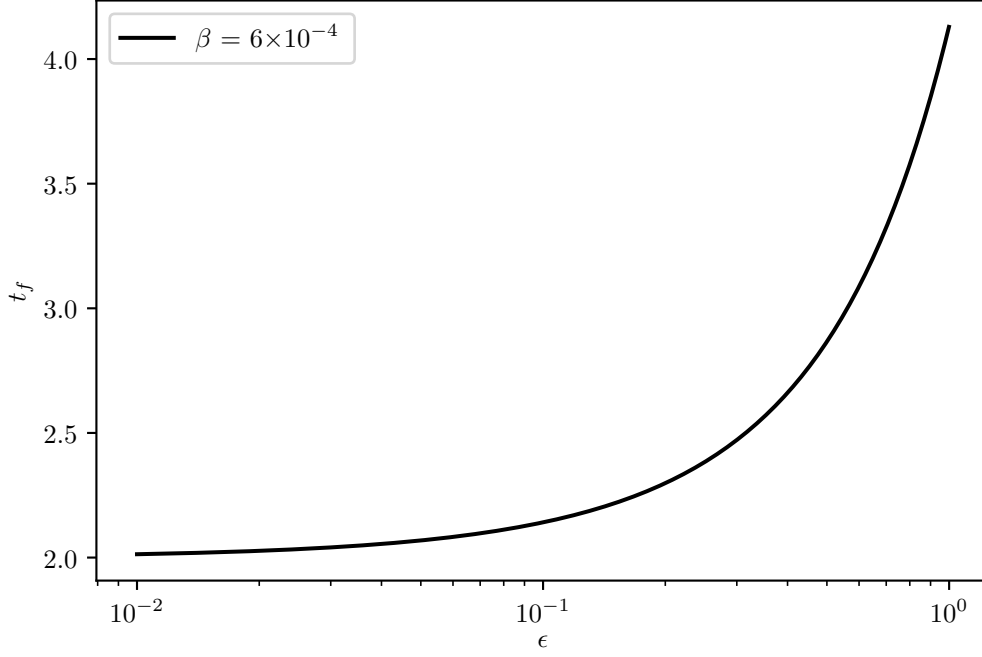
Figure 4: Droplet time-of-flight as a function of $\epsilon = \mathbb{E}\mathrm{u}_+$.

as $\mathcal{O}(\mathbb{E}\mathrm{u}_+) \to \mathcal{O}(1)$; this is an electrostatic escape velocity, U_e. We can find the escape velocity by solving a modified version of the equation of motion,

$$mu' = -\frac{qE_0}{y^2},$$

where $u = \frac{dy}{dt}$ is the droplet velocity. Integrating between the respective limits,

$$m \int_{U_0}^{u(y)} u\,du = -qE_0 \int_{R_d}^{y} \frac{dy}{y^2},$$

which has the solution

$$u(y) = \pm U_0 \left[1 + \frac{2qE_0}{mU_0^2} \left(\frac{1}{y} - \frac{1}{R_d} \right) \right]^{1/2}.$$

17

This equation has an asymptotic velocity, U_∞ at $y = \infty$ which is real if

$$U_0 \geq U_e = \sqrt{\frac{2qE_0}{mR_d}},$$

where U_e is the escape velocity and $U_\infty = \sqrt{U_0^2 - U_e^2}$. The condition for the droplets to escape the electric field is then given by

$$\mathbb{E}\mathrm{u}_+ > 1/8\pi. \tag{17}$$

If the droplet escapes the electric field it will have a residual velocity U_∞, and will be in a regime of pure inertia $\sim$ drag. The velocity will then decay as

$$\bar{u}(\bar{t}) = \frac{1}{\bar{t} + 1},$$

with a characteristic time $t_c \sim \frac{2m}{C_D \rho A U_\infty}$, which is the halving time of the velocity.

References

[1] F. F. Abraham, "Functional dependence of drag coefficient of a sphere on reynolds number", The Physics of Fluids **13**, 2194–2195 (1970).

[2] D. A. Saville, "ELECTROHYDRODYNAMICS:the taylor-melcher leaky dielectric model", Annual Review of Fluid Mechanics **29**, 27–64 (1997).

[3] K. Yatsuzuka, Y. Mizuno, and K. Asano, "Electrification phenomena of pure water droplets dripping and sliding on a polymer surface", Journal of Electrostatics **32**, 157–171 (1994).

[4]J. R. Melcher, *Continuum electromechanics / james r. melcher*, Includes index. (MIT Press, Cambridge, Mass).

[5]M. Hurwitz, "Electrohydrodynamic propellant management systems for cryogenic upper stages", in *3rd annual meeting*, 0 vols., Annual Meeting, DOI: 10.2514/6.1966-922 DOI: 10.2514/6.1966-922 (American Institute of Aeronautics and Astronautics, Nov. 29, 1966).

[6]H. A. Pohl, "Some effects of nonuniform fields on dielectrics", Journal of Applied Physics **29**, 1182–1188 (1958).

[7]X. Wang, X.-B. Wang, and P. R. C. Gascoyne, "General expressions for dielectrophoretic force and electrorotational torque derived using the maxwell stress tensor method", Journal of Electrostatics **39**, 277–295 (1997).

[8]David J. Griffiths, *Introduction to electrodynamics*, in collab. with Internet Archive (Prentice Hall, 1999), 602 pp.